

## Excitons confined by split-gate potentials

Gregorio H. Coccoletzi\* and Sergio E. Ulloa

*Department of Physics and Astronomy and Condensed Matter and Surface Sciences Program,  
Ohio University, Athens, Ohio 45701-2979*

(Received 28 September 1993)

Quasi-one-dimensional excitons in a GaAs-Al<sub>x</sub>Ga<sub>1-x</sub>As quantum well are studied; they are produced by an applied twin-split-gate potential which confines the particles laterally and allows free motion in one dimension. A variational approach is used to calculate the binding energies  $E_{ex}$  and oscillator strength  $f_{ex}$  of these excitonic transitions as functions of the applied voltage and width of the induced potential wells. In the limit of high electrostatic confinement the excitons are strongly polarized and the system resembles a type II structure where electron and hole are spatially separated. The resulting  $E_{ex}$  and  $f_{ex}$  show a strong dependence on applied voltage and structure width. Strong oscillations are found, which should be observed experimentally, as a consequence of subtle competition between confinement and Coulomb attraction.

The study of elementary excitations in solid state systems has been an interesting subject for many years. Particular attention has been paid lately to the case of confined excitonic transitions in semiconductor heterostructures.<sup>1</sup> Theoretical studies of the oscillator strength  $f_{ex}$  and the binding energies  $E_{ex}$  of the excitonic transitions in single quantum wells,<sup>2-4</sup> coupled quantum wells,<sup>5-8</sup> quantum boxes,<sup>9</sup> and dots<sup>10</sup> have shown that both  $f_{ex}$  and  $E_{ex}$  exhibit strong enhancement as confinement increases. Effects of applied external electric<sup>5</sup> and magnetic<sup>11</sup> fields on the confined excitons also have been investigated. Photoluminescence experiments have demonstrated that excitonic transitions indeed show these effects in single<sup>12</sup> and coupled quantum wells,<sup>13</sup> quantum boxes, and dots.<sup>14</sup> Indeed, confinement effects together with applied fields may allow for easily modulated and well-defined excitonic transitions even at room temperatures. The interest in studying these systems is driven in great part by the intrinsic fundamental processes in quantum structures but also by their possible applications in electro-optical devices.<sup>1</sup>

In this paper, we report binding energies and oscillator strengths of the quasi-one-dimensional (1D) excitonic transitions produced by applied split-gate potentials which confine 2D excitons laterally. Split gates have been used successfully in the study of transport and optical properties of confined electron- or hole-doped systems,<sup>15</sup> but little has been done with intrinsic systems. We anticipate, however, that it is now possible to realize systems where confinement of excitons is "easily" varied by a split gate potential. In particular, one can imagine being able to produce a periodic electric-field modulation by a set of finger or grating gates, and vary the photoluminescent response of the system accordingly. In this work, we explore perhaps the simplest, and yet nontrivial, of such systems. An otherwise 2D-exciton region is modulated by a twin set of split gates, producing localization of the exciton to a quasi-1D geometry, in addition to a strong Stark-like polarization. Indeed, recent work by the LMU-Munich group shows that this type of struc-

tures is within experimental reach already and for rather small period modulation ( $\approx 250$  nm).<sup>16</sup>

We investigate the effects of this electrostatic confinement on the optical properties of these systems by following a familiar variational approach similar to that of Dignam and Sipe<sup>5</sup> and others.<sup>8,11</sup> The variational wave function of the exciton is written as the product of a function depending on the relative coordinates of the system, and the single-particle wave functions of the individual electron and hole appropriate for the specific geometry of interest. In the limit of strong electrostatic confinement, the situation studied here resembles the excitons in type II quantum-wells,<sup>17</sup> where the electron and hole are confined in spatially separated wells. We obtain, correspondingly, that the applied potential and the lateral confinement significantly affect  $E_{ex}$  and  $f_{ex}$  as compared to the free and 2D exciton cases. In fact, we find interesting oscillations in these quantities with changes of the various parameters describing the system. These oscillations are due to a subtle interplay between particle confinement and the Coulomb interaction defining the exciton.

To focus ideas, we model a quantum-well structure of GaAs-Al<sub>x</sub>Ga<sub>1-x</sub>As with a corresponding twin split-gate configuration, as depicted in Fig. 1. The excitons are confined in the  $z$  direction by a quantum well of width  $a_3$  (structural confinement) and in the  $x$  direction by the gate potential (electrostatic confinement), while they are free to move along the  $y$  direction. Our main interest is to investigate the effects of the electrostatic confinement on the binding energies  $E_{ex}$  and oscillator strength  $f_{ex}$  of the excitonic transitions. We proceed by writing the Schrödinger equation in the effective mass approximation and neglect any band nonparabolicity, as we deal with typically small excitonic energies. The Hamiltonian of the excitons in the potential configuration under study can be written as  $H = H_0 + V^e + V^h$ , where  $H_0 = T - e^2/\epsilon r$ ,  $T$  is the kinetic energy operator for both electron and hole,  $\epsilon$  is the static dielectric constant,  $r$  is the relative electron-hole coordinate, and

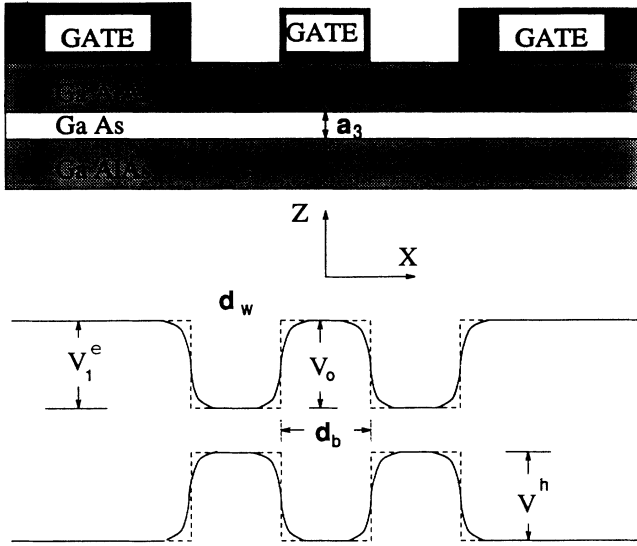


FIG. 1. Schematic cross-sectional view of structure. Bottom traces sketch *effective potentials* for electrons and holes in the GaAs region (rather than band-edge profiles). Dashed square profile of Eq. (1) used in the calculations is uniform along the  $y$  direction.

$$V^e(x_e) = \begin{cases} V_1^e, & |x_e| \geq d_w + d_b/2 \\ V_0^e, & |x_e| \leq d_b/2 \\ 0 & \text{otherwise.} \end{cases} \quad (1)$$

The corresponding effective potential for holes (up to a constant) is  $V^h(x_h) = -V^e(x_e \rightarrow x_h)$ , as the source of the modulation is electrostatic and only the charge sign is different for both carriers. Notice that we approximate the most-likely rounded smooth potential function  $V^e(x_e)$  by a sequence of square profiles. We anticipate this to have no qualitative consequences in our conclusions below. (Note that Fig. 1 shows the *effective potentials* seen by the electron and hole, rather than the band edge profiles.)

To calculate  $E_{\text{ex}}$  and  $f_{\text{ex}}$  with the above Hamiltonian we follow a procedure similar to that used by Dignam and Sipe for coupled quantum wells in 2D.<sup>5</sup> We write the Hamiltonian of a single well potential  $V_i^e$  for the electrons (either the left or right well), and the shifted central potential well for the holes  $V^h$ , as  $H_i = H_0 + V_i^e + V^h$ . The corresponding variational solution is then written as

$$\Psi_i(\mathbf{r}_e, \mathbf{r}_h) = \frac{c_0}{\lambda} e^{-r/\lambda} \psi_i(\mathbf{r}_e, \mathbf{r}_h), \quad (2)$$

with

$$\psi_i(\mathbf{r}_e, \mathbf{r}_h) = \psi(\rho_e, \rho_h) f_i^e(x_e) f^h(x_h), \quad (3)$$

$\mathbf{r}_j = (x_j, \rho_j)$ ,  $j = e, h$ , and  $r = |\mathbf{r}_e - \mathbf{r}_h|$ . In this equation,  $f_i^e$  and  $f^h$  are the wave functions of the electron and hole for the isolated wells, respectively. The expressions we use are (for each well centered at the origin)

$$f^j = \begin{cases} Ae^{\alpha x_j}, & x_j \leq -d_j/2 \\ B \cos(k^j x_j), & |x_j| \leq d_j/2 \\ Ce^{-\tau x_j}, & x_j \geq d_j/2, \end{cases} \quad (4)$$

where  $d_j$  is the potential well width,  $k^j = \sqrt{2m_j E_j / \hbar^2}$  is the particle wave vector in the isolated well, and  $\psi(\rho_e, \rho_h) = D \cos(q_{ze} z_e) \cos(q_{zh} z_h) e^{i(q_{ye} y_e + q_{yh} y_h)}$ . Here,  $\lambda$  is the only free variational parameter, as  $k^j$  is determined from the solution of the finite quantum well in the  $x$  direction,  $q = \pi/a_3$  is the wave vector in the  $z$  direction, and the constants  $\alpha$  and  $\tau$ , as well as  $A$  to  $D$ , are calculated using the boundary and the normalization conditions of the wave function for the single-well problem. Full confinement in the  $z$  direction has been assumed for simplicity, and can be relaxed for a detailed comparison with experiments, but introduces no qualitative changes in our results that deal with the *lateral* confinement effects.

Using the single-well Hamiltonian  $H_i$ , we can write the full Hamiltonian as  $H = H_i + \Delta_i$ , where the only nonzero values of  $\Delta_i$  are  $\Delta_1 = -V_1^e$ , for  $d_b/2 \leq x_e \leq d_b/2 + d_w$ , and  $\Delta_2 = -V_1^e$ , for  $-(d_w + d_b/2) \leq x_e \leq -d_b/2$ . This clever procedure allows one to deal with a single variational parameter but with an overall wave function which is adapted well to the physical problem at hand.<sup>5</sup> The full variational solution is now written as the linear combination,  $\Phi = \sum_i b_i \Psi_i$ , where  $\Psi_i$  is given by Eq. (2) for each one of the two wells. The energy is then the expectation value of the Hamiltonian, so that  $\langle \Phi | H | \Phi \rangle = E \langle \Phi | \Phi \rangle$ , and since we are working with a nonorthogonal basis, we solve a  $2 \times 2$  generalized eigenvalue problem. Finally, the binding energies are obtained using the expression  $E_{\text{ex}} = E_{\text{ni}} - E$ , where  $E_{\text{ni}}$  is the energy eigenvalue of the *noninteracting* but still confined electron-hole system.

Similarly, the oscillator strength intensity of the excitonic transitions is estimated from

$$f_{\text{ex}} = \frac{2P^2}{m_0 E} \left| \int \Phi(\mathbf{r}_e, \mathbf{r}_e) d\mathbf{r}_e \right|^2, \quad (5)$$

as obtained in the envelope function approximation.<sup>9,18</sup> In this expression  $m_0$  is the bare electron mass and  $P$  is the momentum matrix element between conduction and valence band states.

The parameters used for the actual calculations correspond to a GaAs-Al<sub>x</sub>Ga<sub>1-x</sub>As heterostructure, so that we take  $P^2/m_0 = 1$  eV,  $m_e = 0.067m_0$ ,  $\epsilon = 12.2$ ,  $E_g = 1.52$  eV, and for the heavy hole mass  $m_h^H = 0.377m_0$ .<sup>1</sup> The results for the light-hole exciton will be reported elsewhere, as well as the possible mixing of light and heavy holes under these conditions, as these points do not add qualitative features to our discussion. Notice also that we ignore here possible finite trapping lifetime effects for the hole, especially important for the light hole, as it could more easily tunnel out of the electrostatically defined well in Fig. 1. In other words, we assume that the exciton lifetime is shorter than the escaping or tunneling-out time.

As the gate potentials are varied, one can effectively change several structural parameters of the model such as the width of the potential wells ( $d_w$  for electrons and  $d_b$  for holes), the width  $d_b$  of the potential barrier for the electrons, and the asymptotic height  $V_1^e$  of the applied potential. Moreover, the  $z$  width of the quantum well  $a_3$  is also readily changed by different sample GaAs thicknesses. To examine the effects of electrostatic confine-

ment, we calculate the binding energies  $E_{\text{ex}}$  and the oscillator strength  $f_{\text{ex}}$  of the excitonic transitions as functions of the electronic well width  $d_w$ , for different values of  $d_b$  and the barrier height. For simplicity, we assume further that  $V_1^e = V_0$ . The energies are given in terms of the exciton effective Rydberg [ $= \mu e^4 / 2\hbar^2 \epsilon^2 = \text{Ry}^* = 5.2 \text{ meV}$ ;  $\mu = (m_e^{-1} + m_h^H)^{-1} = 0.057 m_0$ ], and all the lengths in terms of the exciton Bohr radius ( $= a_0 = \epsilon \hbar^2 / \mu e^2 = 110 \text{ \AA}$ ).

We discuss the effects of electrostatic confinement on  $E_{\text{ex}}$  and  $f_{\text{ex}}$ , considering two regimes. In the first case, we take  $V_0$  to be a constant ( $= 10 \text{ Ry}^*$ ), as we vary  $d_w$ . This would correspond approximately to changing the voltage on the side gates while keeping the central one constant. We consider different values of  $d_b$ . In the second case, we keep  $d_b$  constant ( $= 2a_0$ ) and allow  $V_0$  to have different values. For simplicity, we maintain  $a_3 = 0.45a_0 \approx 50 \text{ \AA}$  constant in the figures below.

Figure 2 shows typical results for  $E_{\text{ex}}$  and  $f_{\text{ex}}$  versus electron well width  $d_w$  (see Fig. 1). Generally stronger binding occurs for a system with smaller  $d_b$  ( $= a_0$ ), as the electron and hole are allowed to coexist in the same region [the barrier (well) region for the electron (hole)]. The binding is generally smaller for larger  $d_b$ , as this forces the electron out of the barrier. Correspondingly, the oscillator strength — which depends strongly on the electron-hole overlap — decreases rapidly for weaker binding (by as much as an order of magnitude for only a factor of two drop in  $E_{\text{ex}}$ ). The variational parameter  $\lambda$  is also generally smaller for weaker binding; see the inset. Notice that  $\lambda$  characterizes the effective size of the exciton, as seen in Eq. (2), and one can easily verify numerically that  $\langle r \rangle \approx \lambda$  (not shown). [Incidentally, although the trial wave function is not explicitly symmetric in  $x$  and

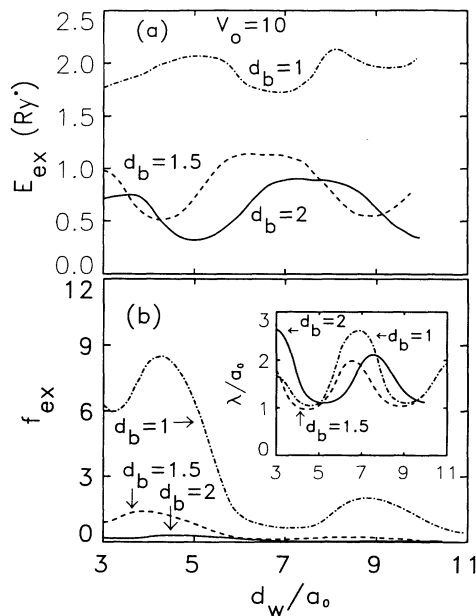


FIG. 2. Binding energy  $E_{\text{ex}}$  and oscillator strength  $f_{\text{ex}}$  versus well-width  $d_w$ , for various  $d_b$  values as shown (in units of  $a_0$ ). Inset in (b) shows the resulting exciton size  $\lambda$  for each case.  $V_0 = 10 \text{ Ry}^*$  in all traces.

$y$ , the resulting ground state exhibits this symmetry to first order, in that  $\langle |x| \rangle \approx \langle |y| \rangle$ , making for a nearly “circular” exciton (with  $\langle |z| \rangle \approx 0$ .)

We see also in Fig. 2 that for all three values of the hole well width  $d_b$  shown, the binding energy oscillates strongly with  $d_w$ . These oscillations cease for systems with  $d_b \geq 5a_0$ , approximately. The oscillations are somewhat surprising, as one would expect that a smaller  $d_w$  would confine the exciton further and increase  $E_{\text{ex}}$  rather *monotonically*. This is indeed what happens as a 3D exciton is confined to 2D,<sup>12</sup> or a 2D to 1D.<sup>9</sup> Notice, however, that this behavior occurs for a “direct” exciton, where electron and hole coexist spatially. This is not the case here, at least for large  $d_b$  and/or  $V_0$  values, as the exciton is polarized and the electron and hole are forced into different wells. This is further corroborated by careful inspection of Fig. 2: For  $d_b/a_0 = 1$ , the most nearly-direct exciton shown here,  $\lambda$  increases as  $E_{\text{ex}}$  decreases vs  $d_w$ , and vice versa. This is in agreement with the intuitive idea that as the exciton becomes larger, the binding decreases. However, for the other two cases shown with larger  $d_b$ , although smaller than  $d_b \approx 5a_0$ ,  $\lambda$  is *in phase* with  $E_{\text{ex}}$ , increasing or decreasing simultaneously. This behavior is understood if one considers that the binding energy measures not only the effect of the Coulomb interaction (which is the origin of the “out-of-phase” behavior of  $\lambda$  vs  $E_{\text{ex}}$  for  $d_b = a_0$ ) but also the change in kinetic energy incurred as the electron and hole “pull on each other” and deform the noninteracting wave functions to be closer to the barrier. Correspondingly, the negative curvature component of this bound state coming from the barrier region for the electron is larger than that of the noninteracting case, overtaking the size increase in Coulomb energy. Notice that this behavior is the result of a rather subtle cancellation since as the electron-hole overlap increases due to the Coulomb attraction, so does

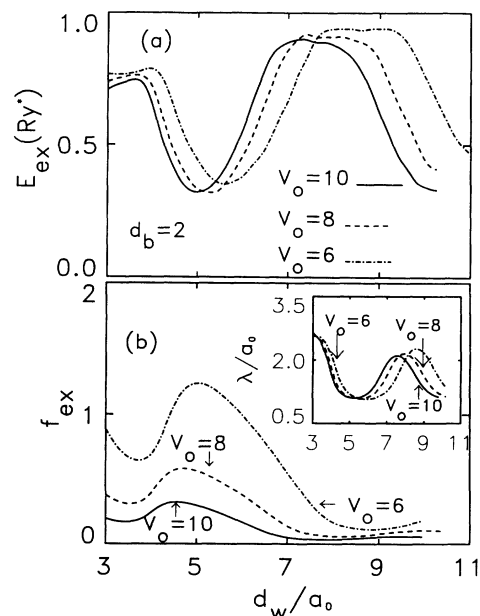


FIG. 3. Same as Fig. 2 but with  $d_b = 2a_0$  fixed, for various  $V_0$  values.

the weight of the electron on the barrier and the corresponding potential energy cost. This latter increase eventually dominates and the binding energy decreases. This competition between the various terms can be seen explicitly in plots of the kinetic energy and Coulomb energy changes vs  $d_w$  (plots not shown here). Since  $V_{\text{Coulomb}} \approx \langle 1/r \rangle$  (which follows closely  $\langle r \rangle^{-1} \approx \lambda^{-1}$ ), this term varies out of phase with  $\lambda$ . The kinetic energy term variations can be seen to compensate this change, giving rise to the binding energy curves in Figs. 2 and 3.

Next we explore the effects of different applied potentials on  $\lambda$ ,  $E_{\text{ex}}$ , and  $f_{\text{ex}}$ . We take  $d_b = 2a_0$  and, as such, Fig. 3 shows small binding energies ( $\approx 1 \text{ Ry}^*$ ) for three values of  $V_0$ . The curves have similar behavior, with a shift to higher values as the applied potential decreases. Since the barrier is rather wide, and the electron-hole overlap is small, the sensitivity to  $V_0$  is not significant. In all cases too, the variational parameter  $\lambda$  varies in phase with  $E_{\text{ex}}$ , indicating further that the exciton is basically spatially indirect (see inset). Similarly, the oscillator strength shows oscillations on an overall decaying tail as  $d_w$  increases. Notice that  $f_{\text{ex}}$  decreases rapidly as  $V_0$  increases because of its exponential dependence on the electron-hole overlap.

In conclusion, we have presented a study of the quasi-1D excitonic transitions in quantum wells in the pres-

ence of lateral electrostatic confinement. We have used a variational approach to calculate the binding energies, oscillator strength, and the effective exciton size. For the case of strong confinement but small or thin middle barrier, we find that the energies  $E_{\text{ex}}$  and the oscillator strength are greatly enhanced with respect to those of the free excitons, as the resulting potential yields nearly spatially direct excitons. As the middle barrier increases its width or size the exciton polarizes, electron and hole separate, and  $E_{\text{ex}}$  and  $f_{\text{ex}}$  decrease significantly. We also find strong oscillations in these quantities as the well-width is varied, which appear as the result of interesting cancellations between Coulomb attraction and particle confinement. Given the strong signatures associated with these effects, we expect that all of these features should be observable in experiments where such a split-gate geometry is implemented.

S.E.U. acknowledges helpful discussions with W. Hansen and A. Schmeller on their interdigitated gated structures. G.H.C. acknowledges the financial support of CONACyT-México. This research was supported by the U.S. Department of Energy, Grant No. DE-FG02-91ER45334. Calculations were performed on the Cray Y/MP at the Ohio Supercomputer Center, under project No. PHS060.

\*Permanent address: Centro de Investigaciones en Dispositivos Semiconductores, Instituto de Ciencias, Universidad Autónoma de Puebla, Apartado Postal 1651, Puebla 72000, Mexico.

<sup>1</sup>See, for example, G. Bastard, J. A. Brum, and R. Ferreira, in *Solid State Physics: Advances in Research and Applications*, edited by H. Ehrenreich and D. Turnbull (Academic, San Diego, 1991), Vol. 44, p. 229.

<sup>2</sup>J. A. Brum and G. Bastard, *J. Phys. C* **18**, L789 (1985).

<sup>3</sup>Y. Shinozuka and M. Matsuura, *Phys. Rev. B* **28**, 4878 (1983).

<sup>4</sup>R. L. Greene, *Phys. Rev. B* **29**, 1807 (1984).

<sup>5</sup>M. M. Dignam and J. E. Sipe, *Phys. Rev. B* **43**, 4084 (1991).

<sup>6</sup>J. Lee, M. O. Vassell, E. S. Koteles, and B. Elman, *Phys. Rev. B* **39**, 10 133 (1989).

<sup>7</sup>F. M. Peeters and J. E. Golub, *Phys. Rev. B* **43**, 5159 (1991).

<sup>8</sup>G. W. Bryant, *Phys. Rev. B* **46**, 1893 (1992).

<sup>9</sup>G. W. Bryant, *Phys. Rev. B* **37**, 8763 (1988).

<sup>10</sup>W. Que, *Phys. Rev. B* **45**, 11 036 (1992).

<sup>11</sup>J. Cen and K. K. Bajaj, *Phys. Rev. B* **46**, 15 280 (1992).

<sup>12</sup>R. C. Miller, D. A. Kleinman, W. T. Tsang, and A. C.

Gossard, *Phys. Rev. B* **24**, 1134 (1981).

<sup>13</sup>Y. J. Chen, E. S. Koteles, B. S. Elman, and C. A. Armiento, *Phys. Rev. B* **36**, 4562 (1987).

<sup>14</sup>K. Kash, A. Scherer, J. M. Worlock, H. G. Craighead, and M. C. Tamargo, *Appl. Phys. Lett.* **49**, 1043 (1986); H. Temkin, G. J. Dolan, M. B. Panish, and S. N. Chu, *ibid.* **50**, 413 (1987); K. Kash, R. Bhat, D. D. Mahoney, P. S. D. Lin, A. Scherer, J. M. Worlock, B. P. Van Der Gaag, M. Koza, and P. Grabbe, *ibid.* **55**, 681 (1989).

<sup>15</sup>See, for example, C. W. J. Beenakker and H. van Houten, in *Solid State Physics: Advances in Research and Applications*, edited by H. Ehrenreich and D. Turnbull (Academic, San Diego, 1991), Vol. 44, p. 1; S. E. Ulloa, A. MacKinnon, E. Castaño, and G. Kirczenow, in *Handbook on Semiconductors*, edited by P. T. Landsberg (Elsevier, Amsterdam, 1992), Vol. 1, p. 863.

<sup>16</sup>A. Schmeller, W. Hansen, J. P. Kotthaus, G. Tränkle, and G. Weimann (unpublished); C. Peters, W. Hansen, J. P. Kotthaus, and M. Holland (unpublished).

<sup>17</sup>M. Matsuura and Y. Shinozuka, *Phys. Rev. B* **38**, 9830 (1988).

<sup>18</sup>R. J. Elliot, *Phys. Rev.* **108**, 1384 (1957).

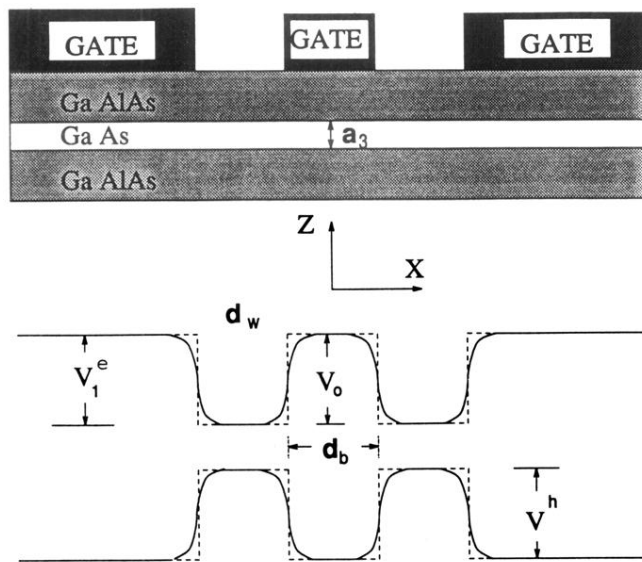


FIG. 1. Schematic cross-sectional view of structure. Bottom traces sketch *effective potentials* for electrons and holes in the GaAs region (rather than band-edge profiles). Dashed square profile of Eq. (1) used in the calculations is uniform along the  $y$  direction.